

# Electrical Insulation Characteristics of HTS Cables Under Quench-Induced Thermal Stress Condition

N. Hayakawa, S. Ueyama, H. Kojima, F. Endo, T. Masuda, and M. Hirose

**Abstract**—This paper discusses the electrical insulation characteristics of high temperature superconducting (HTS) cable under quench condition exposed to thermal and electrical combined stress. We applied a high voltage of 60 Hz ac to the sample electrode, and injected a large current of 60 Hz ac into Bi2223/Ag tapes to induce quench. Experimental results revealed that partial discharges (PD) were induced by the transient thermal stress due to quench under the high voltage condition. A criterion of the combined stress for PD inception was experimentally obtained.

**Index Terms**—Combined stress, electrical insulation, HTS cable, partial discharge, quench.

## I. INTRODUCTION

HIGH temperature superconducting (HTS) cables have higher power density and lower losses than conventional cables. Currently, HTS cables are being installed in the power transmission system, and field tests have been carried out [1].

When a fault current in the power transmission system becomes much higher than the critical current of HTS cables, quench of HTS tapes will be induced together with a large amount of thermal energy. In such a critical condition, transient thermal stress will be superimposed on the electric field stress under operating voltage of HTS cables, which has not been taken into account in the electrical insulation design of HTS cables. Some superconducting fault current limiters have been designed with consideration of such thermal/electrical combined stress being applied to their electrical insulation [2], [3]. Dielectric characteristics of HTS cables under such combined stress should be elucidated for the enhancement of HTS cable reliability.

From the above background, in this paper, we investigated electrical insulation characteristics of HTS cables under quench-induced thermal stress condition. We constructed a test electrode system for high voltage and large current application to simulate the electrical insulation structure of HTS cables.

Manuscript received August 29, 2006.

N. Hayakawa and S. Ueyama are with the Department of Electrical Engineering and Computer Science, Nagoya University, Furo-cho, Chikusa-ku, Nagoya 464-8603, Japan (e-mail: nhayakaw@nuee.nagoya-u.ac.jp; ueyama@okubo.nuee.nagoya-u.ac.jp).

H. Kojima and F. Endo are with the EcoTopia Science Institute, Nagoya University, Furo-cho, Chikusa-ku, Nagoya 464-8603, Japan (e-mail: h-kojima@esi.nagoya-u.ac.jp; endo@sei.nagoya-u.ac.jp).

T. Masuda and M. Hirose are with Sumitomo Electric Industries, 1-1-3, Shimaya, Konohana-ku, Osaka, 554-0024, Japan (e-mail: masuda-takato@sei.co.jp; hirose-masayuki@sei.co.jp).

Color versions of one or more of the figures in this paper are available online at <http://ieeexplore.ieee.org>.

Digital Object Identifier 10.1109/TASC.2007.899968

Through electrical and optical measurements, a criterion of the combined stress level to induce partial discharge (PD) was suggested in the test electrode system.

## II. EXPERIMENTAL SETUP AND PROCEDURE

### A. Experimental Setup

The experimental setup used in this paper is shown in Fig. 1. Fig. 1(a) is the experimental circuit. The cryostat has a capacitor bushing, PD free at 100 kV<sub>rms</sub> in liquid nitrogen, and observation windows installed in four directions. Fig. 1(b) is the test electrode system, and Fig. 1(c) is the HTS tapes (Bi2223/Ag) arrangement.

In order to simulate the electrical insulation structure of HTS cables, three polypropylene laminated papers (thickness: 0.125 mm) without butt gaps were sandwiched between a high voltage plane electrode and grounded Bi2223/Ag tapes with two semi-conducting sheets (thickness: 0.1 mm) by a mechanical pressure. The Bi2223/Ag tapes (critical current  $I_c$ : 100 A, width: 4.1 mm, thickness: 0.22 mm, effective length: 90 mm) have a meander-like shape, as shown in Fig. 1(c), where 8 tapes with the almost identical  $I_c$  were connected in series. The high voltage plane electrode was made of aluminum and molded with epoxy resin to avoid the edge effect. The electrode system was immersed in liquid nitrogen at atmospheric pressure.

### B. Experimental Procedure

As the experimental method, we first carried out the electrical insulation test under ac high voltage without current flow to HTS tapes, in order to know the intrinsic electrical insulation level (static partial discharge inception voltage:  $PDIV_{sta}$ ) of the test electrode system. Secondly, we applied and kept a high voltage  $V_a$  below  $PDIV_{sta}$  of 60 Hz ac to the plane electrode. Thirdly, with exposing the test electrode to a high electric field, quench was induced in the Bi2223/Ag tapes by a large current of 60 Hz ac during 5 cycles, which may induce the partial discharge (PD).

We measured PD signals through an electrical PD detection circuit composed of parallel-connected capacitance and resistance, and recorded them with the current and voltage signals in the oscilloscope. PD detection sensitivity was 3 pC. Such a synthetic test of high voltage and large current was repeated for different applied voltage and current flow.

## III. EXPERIMENTAL RESULTS AND DISCUSSIONS

### A. Quench-Induced PD Phenomena

First of all,  $PDIV_{sta}$  without current flow to HTS tapes was confirmed to be 23 kV<sub>rms</sub> under 60 Hz ac condition. Next, the

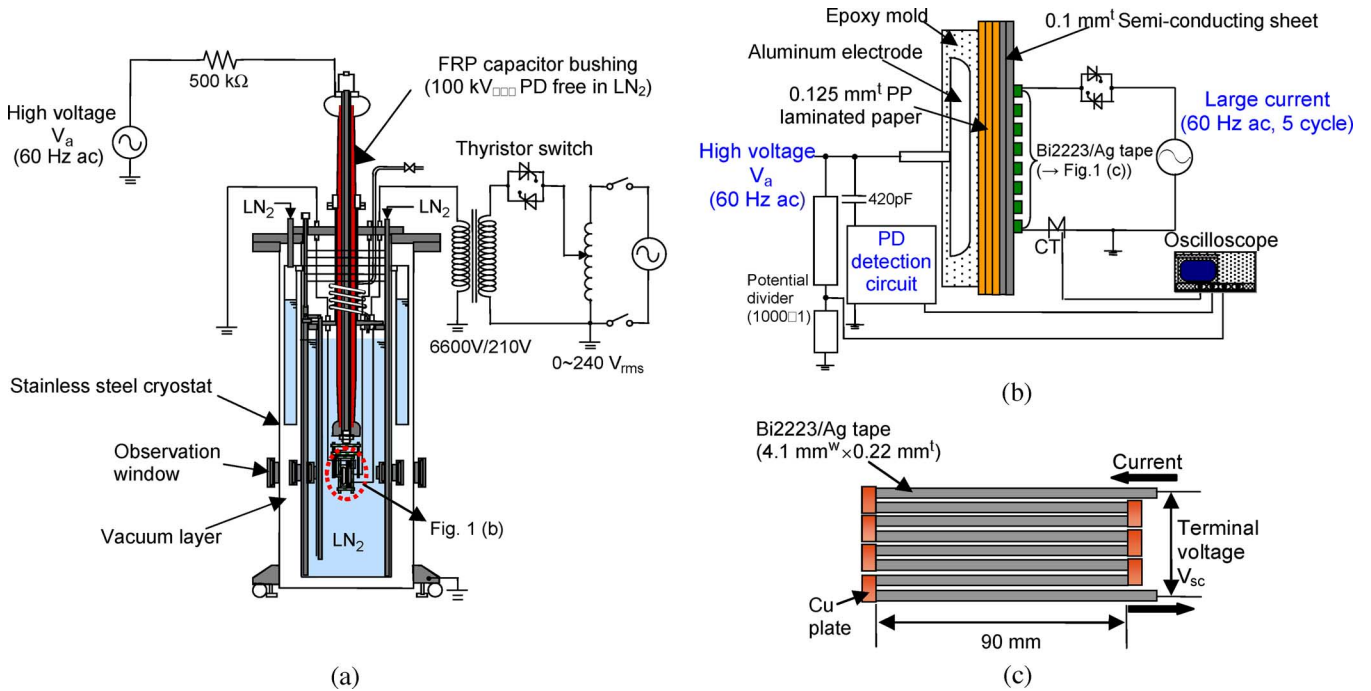


Fig. 1. Experimental setup. (a) Experimental circuit. (b) Test electrode system. (c) Bi2223/Ag tape arrangement.

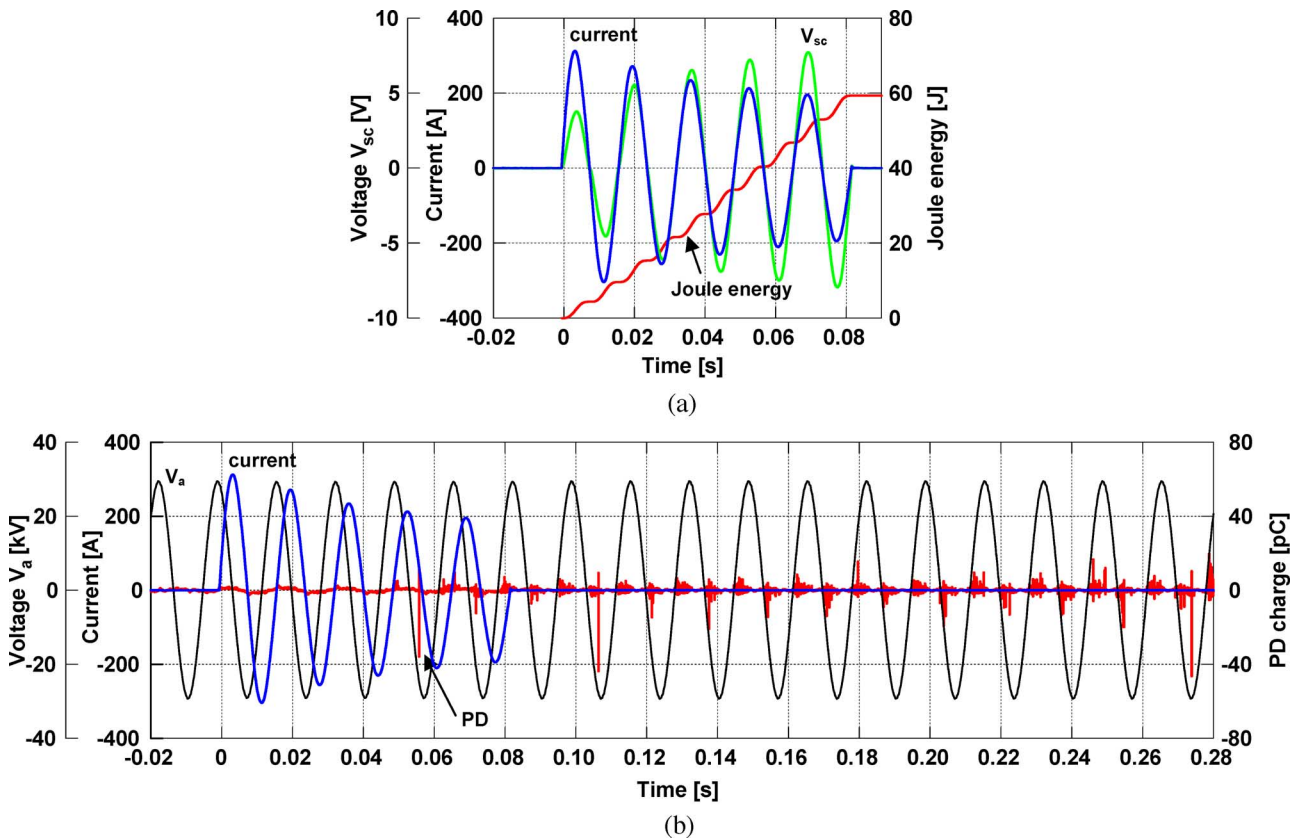
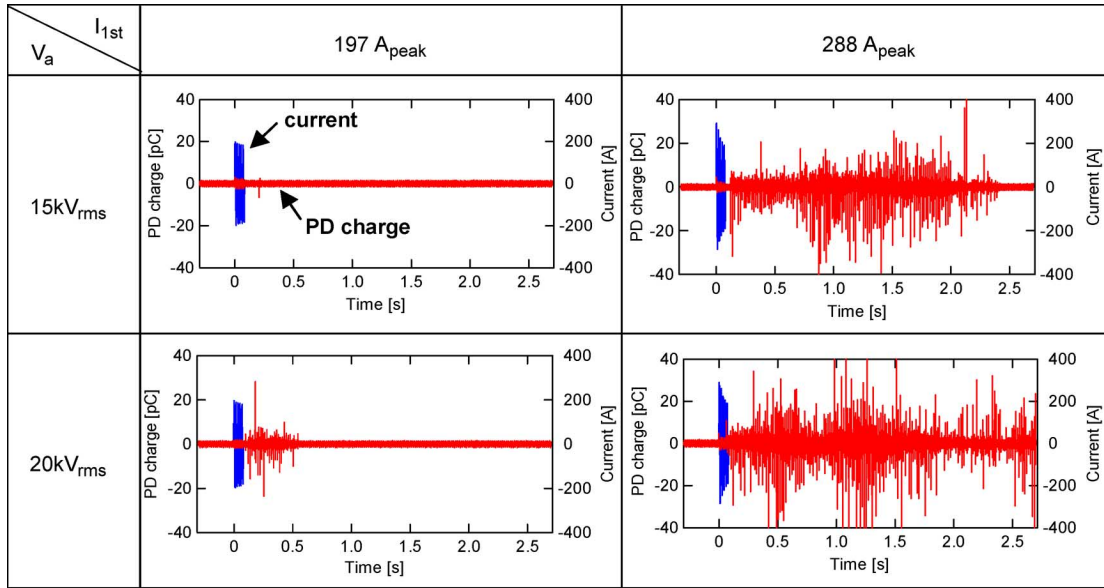


Fig. 2. Quench-induced PD phenomena. (a) Current, voltage and thermal energy waveforms at  $I_{1st} = 308 A_{peak}$ . (b) Quench-induced PD signal at  $V_a = 20 kV_{rms}$  and  $I_{1st} = 308 A_{peak}$ .

synthetic test was carried out. Fig. 2 shows an example at  $V_a = 20 kV_{rms} (= 0.87 \times PDIV_{sta})$  and  $I_{1st} = 308 A_{peak} (= 3.1 \times I_c)$ , where  $I_{1st}$  is the current level at the first peak phase of 60 Hz ac.

Fig. 2(a) shows the current and voltage ( $V_{sc}$ ) waveforms of HTS tapes, where  $V_{sc}$  is the terminal voltage between both ends of the HTS tapes. The current decreased and  $V_{sc}$  increased gradually with time, which means that the quench was induced

TABLE I  
QUENCH-INDUCED PD GENERATION CHARACTERISTICS UNDER THERMAL/ELECTRICAL COMBINED STRESS



in the HTS tapes. As a result, the Joule energy reached about 59 J during 5 cycles.

Fig. 2(b) shows the PD signals with the current and voltage ( $V_a$ ) waveforms. This figure tells us that, in spite of no PD signals before the large current flow even under the high voltage condition, PD was generated by the quench-induced thermal stress in Fig. 2(a). In addition, the voltage phase of PD generation shifted from around peak phase to zero-crossings. This result shows that PD type changed to void-type discharges in the generated bubbles after its inception.

### B. Quench-Induced PD Generation Characteristics

Table I shows PD generation characteristics under thermal/electrical combined stress for different  $V_a$  and  $I_{1st}$ . This table tells us that, at the larger thermal or electrical stress, PD charge, PD number and PD generation duration ( $\Delta t$ : time between the first PD and the last PD) become larger or longer. Fig. 3 shows the PD inception time ( $t_{1st}$ : time between the current injection and the first PD) and  $\Delta t$  as a function of  $V_a$  for different  $I_{1st}$ . This result suggests that  $t_{1st}$  has the tendency to become shorter with the increase in  $V_a$  and  $I_{1st}$ . On the contrary,  $\Delta t$  becomes longer with  $V_a$  and  $I_{1st}$ .

### C. Criterion of Quench-Induced PD Generation

Fig. 4 summarizes the existence of quench-induced PD for different thermal/electrical combined stresses. This figure tells us that a boundary curve of PD generation exists. Moreover, PDIV began to fall by the thermal stress induced by current flow larger than  $I_c$ . PDIV falls remarkably at around  $I_c$  level. Note that, at the current level of  $3 \times I_c$ , PDIV decreased into 8 kV<sub>rms</sub>, i.e. by the factor of 1/3 compared with the static PDIV (23 kV<sub>rms</sub>).

The reasons of these results can be discussed as follows: the quench of HTS tapes induces a large amount of thermal energy. The thermal energy would be transferred into the polypropylene laminated papers through semi-conducting sheets. Then, some

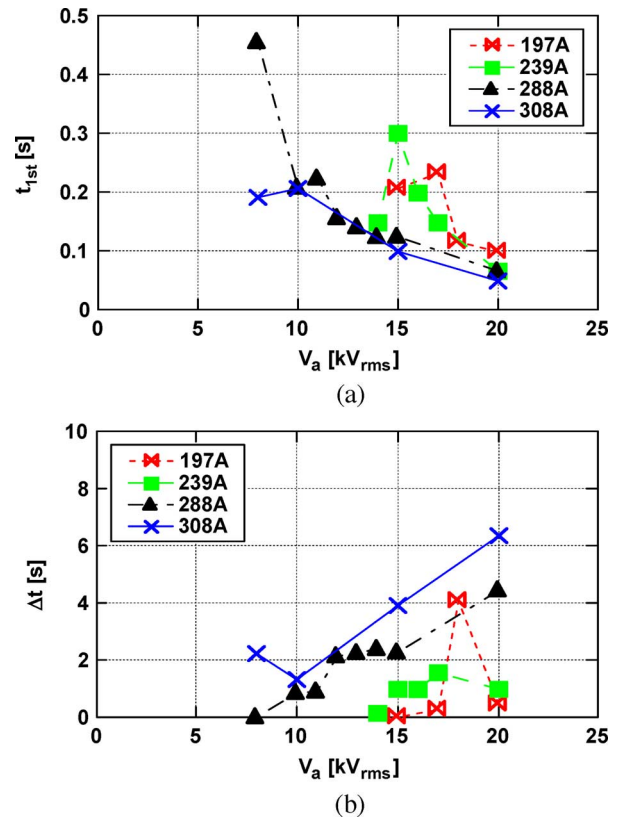


Fig. 3. PD inception time  $t_{1st}$  and PD generation duration  $\Delta t$  as a function of  $V_a$  for different  $I_{1st}$ . (a) PD inception time  $t_{1st}$ . (b) PD generation duration  $\Delta t$ .

weak-points on electrical insulation, e.g. thermal bubbles between paper layers, could be generated in the insulation layer, resulting in the PD generation. The larger thermal or electrical stress can induce more and larger weak-points, and then bring about the reduction of PDIV (Fig. 4), decrease of  $t_{1st}$  (Fig. 3(a)) and increase of  $\Delta t$  (Fig. 3(b)), respectively.

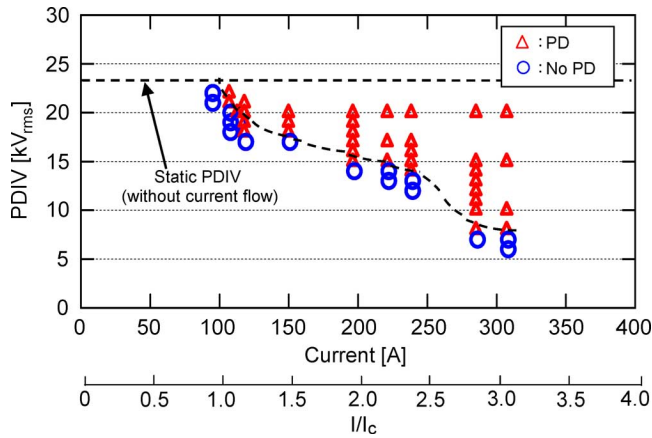


Fig. 4. Criterion of quench-induced PD generation under thermal/electrical combined stress.

*D. Illumination Images of Quench-Induced PD*

In order to verify that PD was generated in the electrical insulation layer, we made an optical PD measurement. In Fig. 1(b), we removed the semi-conducting sheets and replaced the polypropylene laminated paper nearest the HTS tapes with a transparent polypropylene film. PD light emission was observed from the HTS tape side through the observation windows of cryostat using a high-speed video system (200 frames/s) with an image intensifier.

Table II shows the PD light emission images for different  $V_a$  and  $I_{1st}$ . The static PDIV of the optical PD measuring system was 17 kV<sub>rms</sub> due to the difference in the electrode system described above. However, the quench-induced PD phenomena as shown in Fig. 2 were also observed, and the degradation tendency of PDIV against the current flow as shown in Fig. 4 could be basically reproduced. PD light emission in Table II was sporadic after the current flow and expanded in the larger area on the highly electrical-stressed plane with the increase in combined stresses. These optical PD measurements suggest that the quench-induced PD was generated in the highly electrical-stressed region between the transparent polypropylene film and the polypropylene laminated paper or HTS tapes of the test electrode system.

IV. CONCLUSION

This paper described the electrical insulation characteristics under quench-induced thermal and electrical combined stress for HTS cables. The main results are summarized as follows:

TABLE II  
QUENCH-INDUCED PD LIGHT EMISSION IMAGES FOR DIFFERENT  $V_a$  AND  $I_{1st}$

$V_a$ \ $I_{1st}$	196A <sub>peak</sub>	311A <sub>peak</sub>
6kV <sub>rms</sub>		
7kV <sub>rms</sub>		

- 1) Even if the applied high voltage was below the static partial discharge inception voltage (PDIV<sub>sta</sub>), the quench-induced PD could be generated under thermal and electrical combined stress.
- 2) The quench-induced PD generation was activated at the larger thermal and electrical stresses.
- 3) At the current level of  $3 \times I_c$ , PDIV decreased into 8 kV<sub>rms</sub>, i.e. by the factor of 1/3 compared with the static PDIV (23 kV<sub>rms</sub>).
- 4) By the optical PD measurement, the quench-induced PD was verified to occur in the electrical insulation layer of the test electrode system.

REFERENCES

- [1] T. Masuda, H. Yamura, M. Watanabe, H. Takigawa, Y. Ashibe, C. Suzawa, T. Kato, Y. Yamada, K. Sato, S. Isojima, C. Weber, A. Dada, and J. R. Spadafore, "Design and experimental results for Albany HTS cable," *IEEE Trans. Appl. Supercond.*, vol. 15, no. 2, pp. 1806–1809, 2005.
- [2] N. Hayakawa, M. Noe, K.-P. Juengst, and H. Okubo, "Electrical insulation performance under thermal and electric combined stress for resistive superconducting fault current limiters," *IEEE Trans. Appl. Supercond.*, vol. 13, no. 2, pp. 1996–1999, 2003.
- [3] M. Noe, K.-P. Juengst, S. Elschner, J. Bock, F. Breuer, R. Kreutz, M. Kleimaier, K.-H. Weck, and N. Hayakawa, "High voltage design, requirements and tests of a 10 MVA superconducting fault current limiter," *IEEE Trans. Appl. Supercond.*, vol. 15, no. 2, pp. 2082–2085, 2005.